Structure, Volume *20*

Supplemental Information

Proton-Coupled Dynamics in Lactose Permease

Magnus Andersson, Ana-Nicoleta Bondar, J. Alfredo Freites, Douglas J. Tobias, H. Ronald Kaback, and Stephen H. White

Inventory of Supplemental Information

Main Figure	Supplementary Figure	Relationship
1	S1	Supplementary Figure S1 shows the equilibration of the simulated system presented in Figure 1A.
2	S2	Supplementary Figure S2 shows the time-evolution of distances for the charge-pair R144-E126, presented in Figure 2C and F.
2	S3	Supplementary Figure S3 shows a stable charge-pair (D237-K358), which contrasts the interactions shown in Figure 2.
2	S10	Supplementary Figure S10 shows the location of conserved, protonation-sensitive amino acid residues in various MFS transporters of known 3D structure
3	S4	Supplementary Figure S4 shows the time-evolution relative to PDB structure 2V8N for 3 simulations of LacY in POPE and one simulation in DMPC.
3	S5	Supplementary Figure S5 shows structural rearrangements on the cytoplasmic side of LacY, including a pore-radius analysis
5	S6	Supplementary Figure S6 shows structural rearrangements in the proton translocation site
5	S7	Supplementary Figure S7 shows theoretical pKa values for all five simulations computed using the

		program PROPKA
6	**S8**	**Supplementary Figure S8 compares simulated conformational changes to experimental cross-linking data.**
7	**S9**	**Supplementary Figure S9 compares simulations to experimental DEER data**

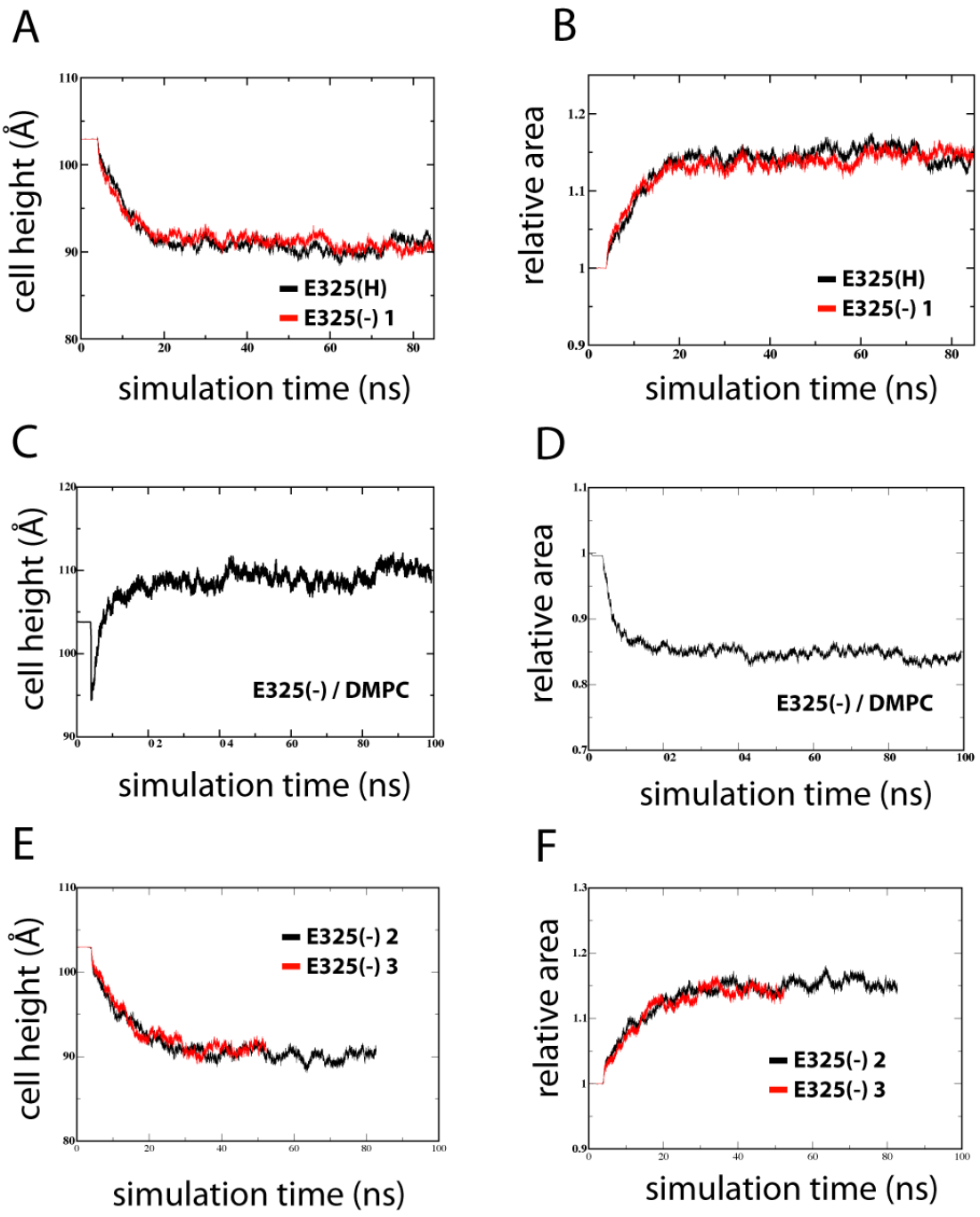

Figure S1, related to Figure 1. Evolution of simulation-cell dimensions. The cell-height of the simulation cell (z-dimension) is displayed for the E325(H) (black) and E325(-) 1 (red) simulation **(A)**, E325(-) / DMPC **(C)**, E325(-) 2 (black) and E325(-) 3 (red) **(E)**. **(B)** The relative area (x,y-dimensions) for these systems are shown in **(B)**, **(D)** and **(F)**.

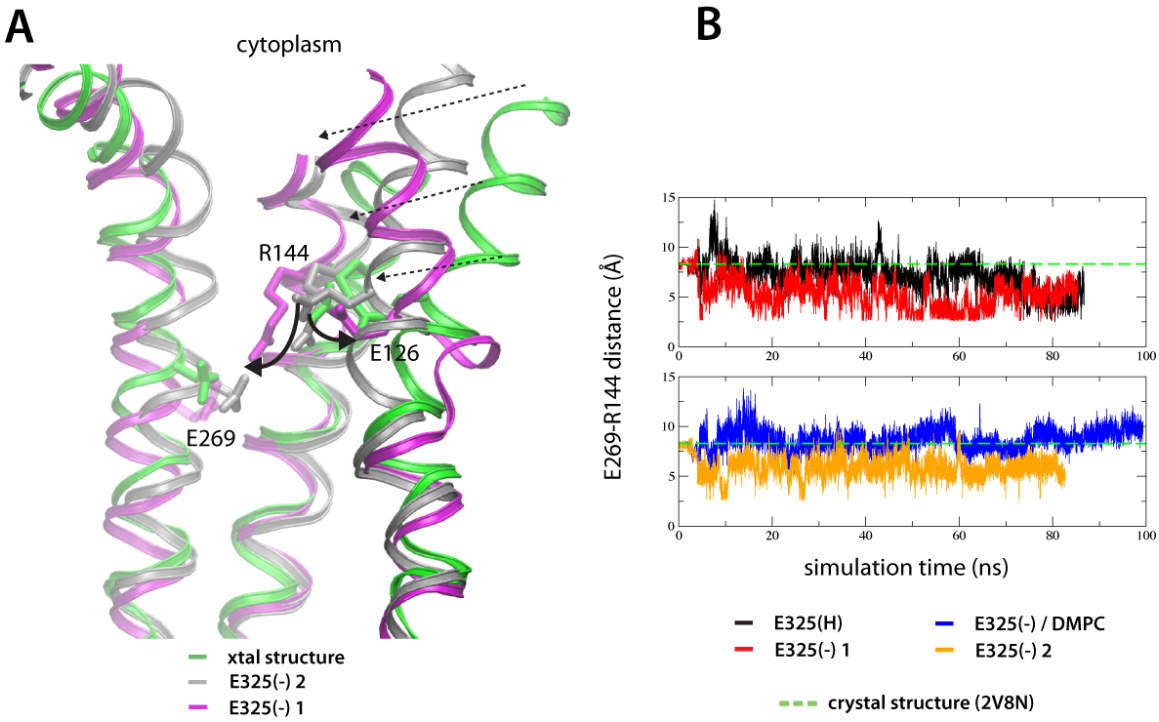

Figure S2, related to Figure 2. Coupling between sidechain dynamics and large-scale conformational changes. **(A)** Last ns averages for E325(-) 1 (magenta) and E325(-) 2 (silver) overlayed on the 2V8N crystal structure. **(B)** E269-R144 inter-atomic distances for the E325(H) (black), E325(-) 1 (red), E325(-) 2 (orange) and E325(-) / DMPC (blue) simulations.

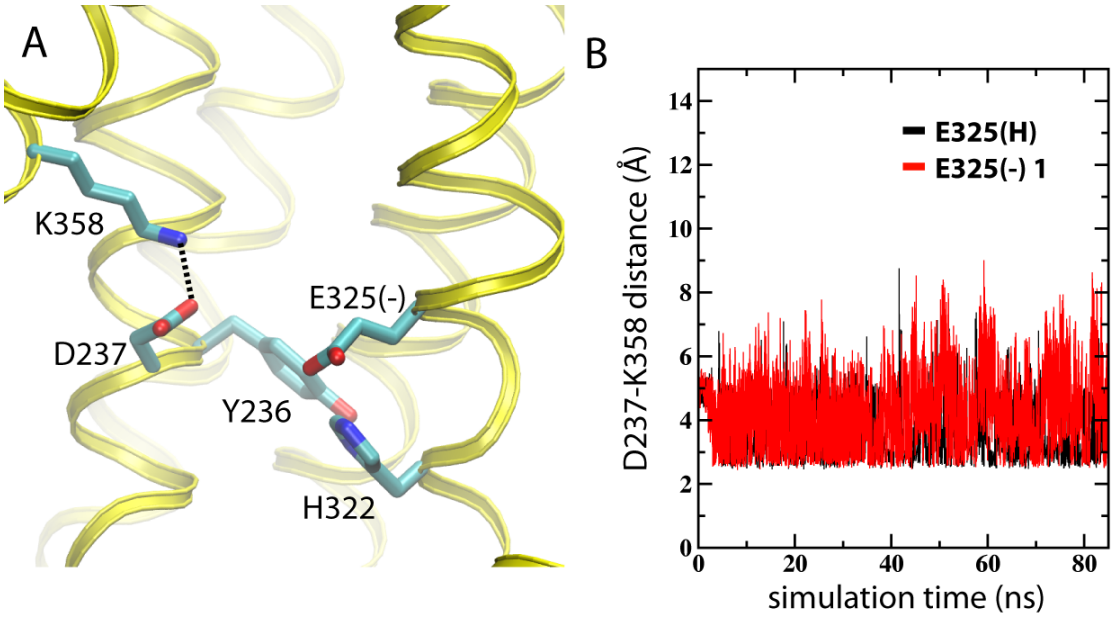

Figure S3, related to Figure 2. The Asp237-Lys358 interaction. **(A)** A snapshot from the E325(-) 1 simulation showing the Asp237-Lys358 interaction and the proximal H^+ translocating site represented by Tyr236, His322 and Glu325. (B) The evolution of the Asp237-Lys358 distance over the trajectory for the E325(H) and the E325(-) 1 in POPE simulation, respectively.

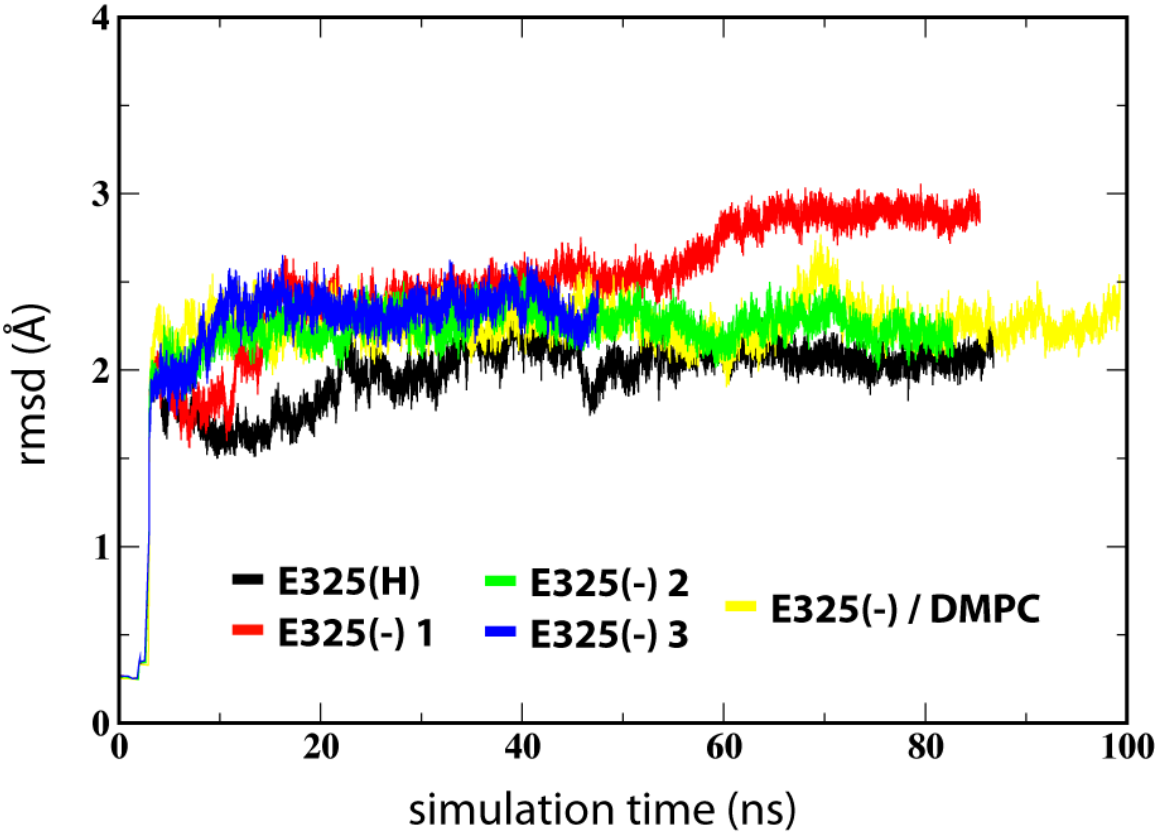

Figure S4, related to Figure 3. RMSD with respect to the 2V8N crystal structure for the E325(H) (black), E325(-) 1 (red), E325(-) 2 (green), E325(-) 3 (blue) and E325(-) / DMPC (yellow) simulations.

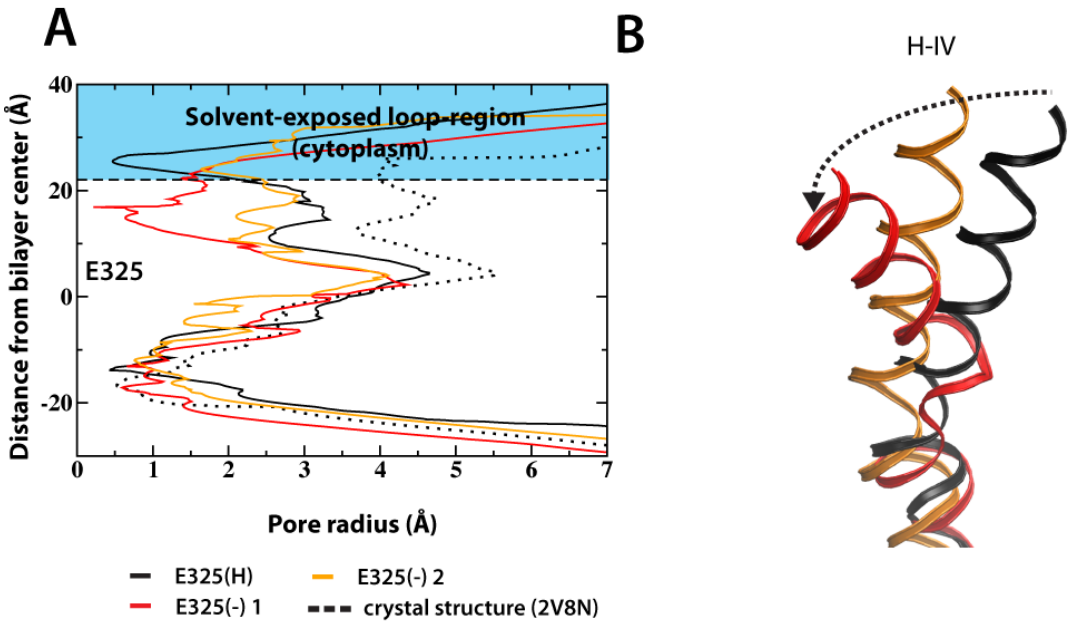

Figure S5, related to Figure 3. Structural rearrangements on the cytoplasmic side of LacY. **(A)** Pore radius analyses using the program HOLE (Smart et al., 1993) of the E325(H) (black), E325(-) 1 (red) and E325(-) 2 (orange) in POPE simulations. The pore radius of the 2V8N crystal structure is depicted as black dots. **(B)** Helix IV from last ns averages of E325(-) 2 (orange) and E325(-) 1 (red) in POPE simulations overlayed on the 2V8N crystal structure (black).

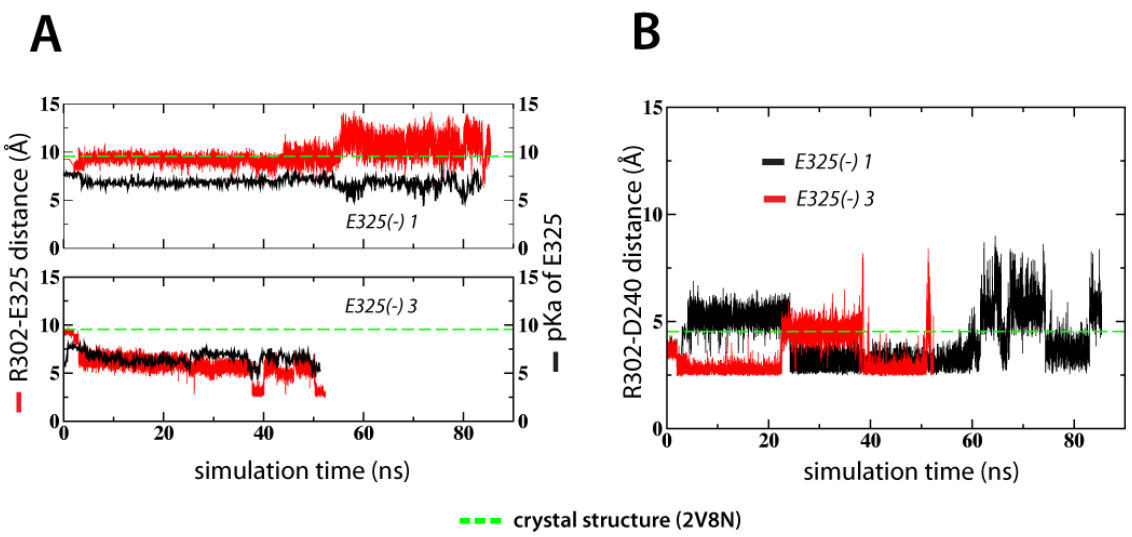

Figure S6, related to Figure 5. Structural rearrangements in the H^+ translocation site. **(A)** Inter-atomic distances between Arg302-Glu325 (red) and calculated Glu325 pKa (black) for the E325(-) 1 and E325(-) 3 simulations, respectively. (B) Arg302-Asp240 inter-atomic distances for the E325(-) 1 (black) and E325(-) 3 (red) simulations, respectively.

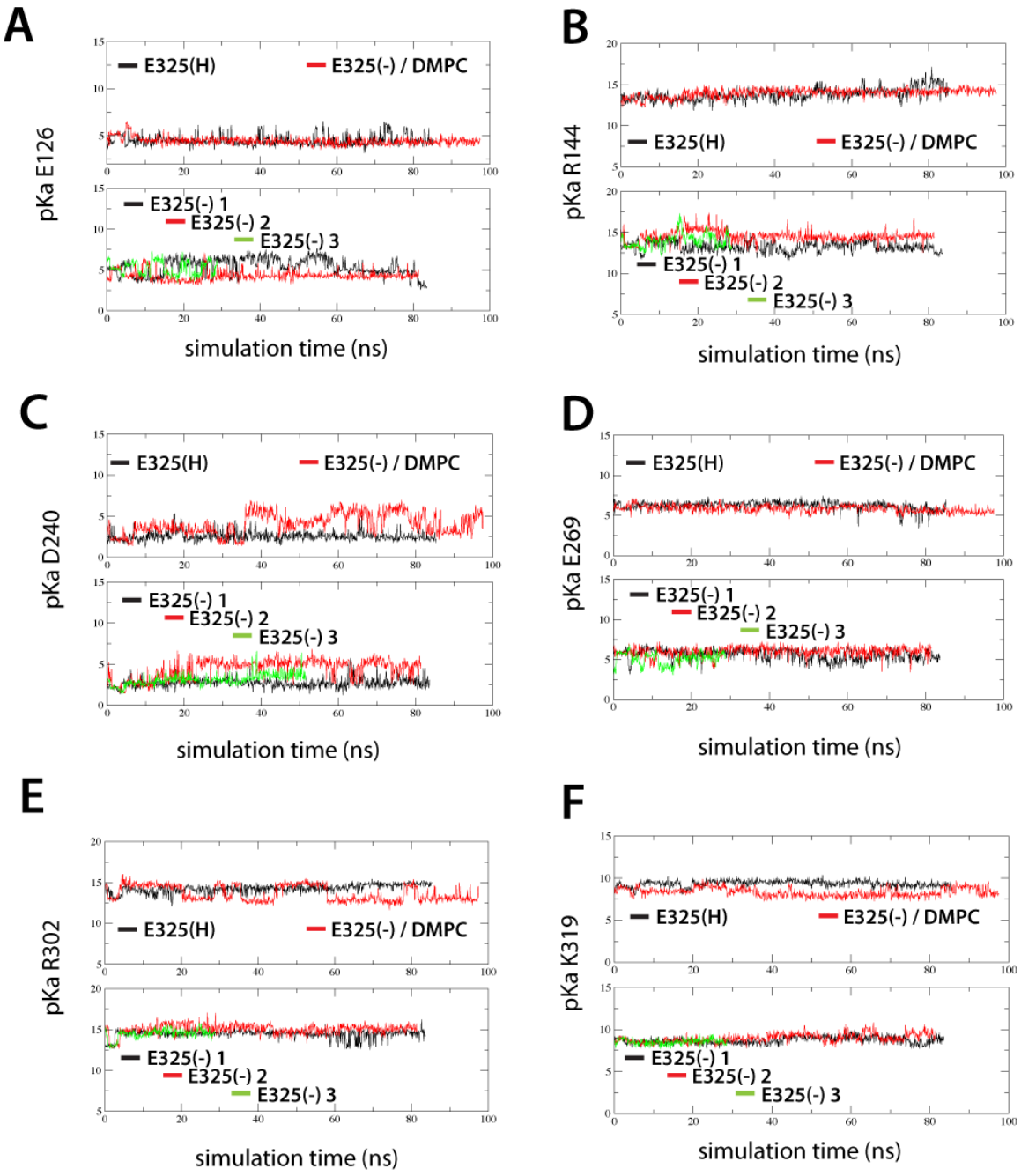

Figure S7, related to Figure 5. Theoretical pKa values (determined for all five simulations by the program PROPKA (Olsson et al., 2011)) for residues involved in H^+ translocation and sugar binding. **(A)** Glu126 **(B)** Arg144 **(C)** Asp240 **(D)** Glu269 **(E)** Arg302 **(F)** Lys319

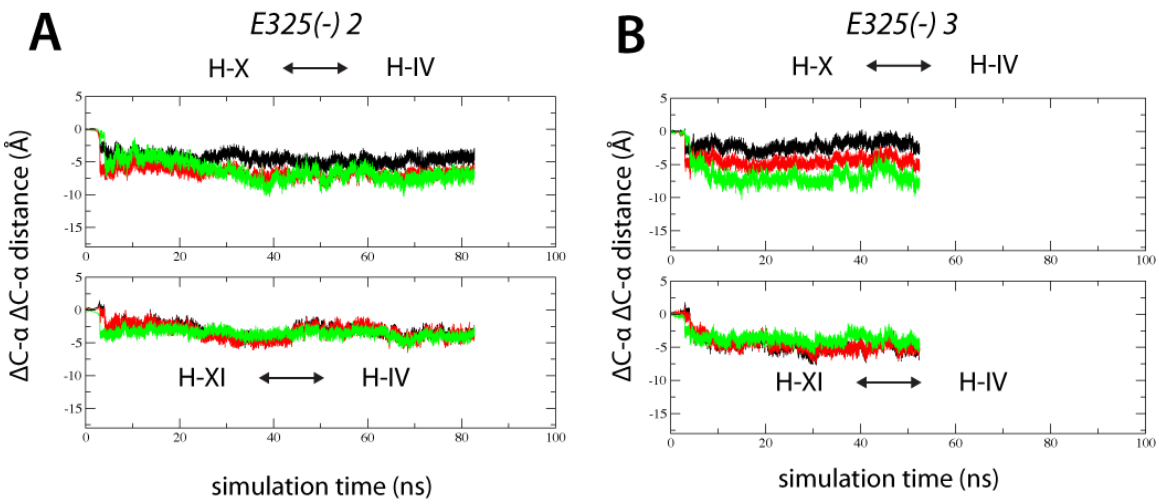

Figure S8, related to Figure 6. Simulated conformational changes related to experimental crosslinking data (Sorgen et al., 2002). The change in distances between Cα in helices IV-X and IV-XI are shown for the E325(-) 2 **(A)** and E325(-) 3 **(B)** simulations, respectively.

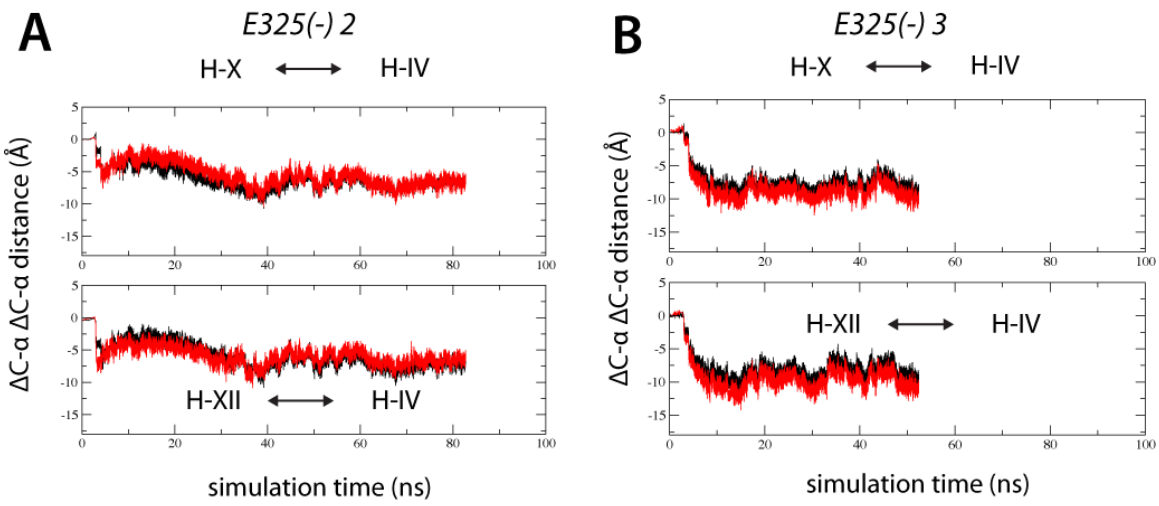

Figure S9, related to Figure 7. Simulated conformational changes in light of experimental DEER data (Smirnova et al., 2007). Changes in Cα-Cα distances between helix IV and either helix X or XII measured from the E325(-) 2 **(A)** and E325(-) 3 **(B)** simulations.

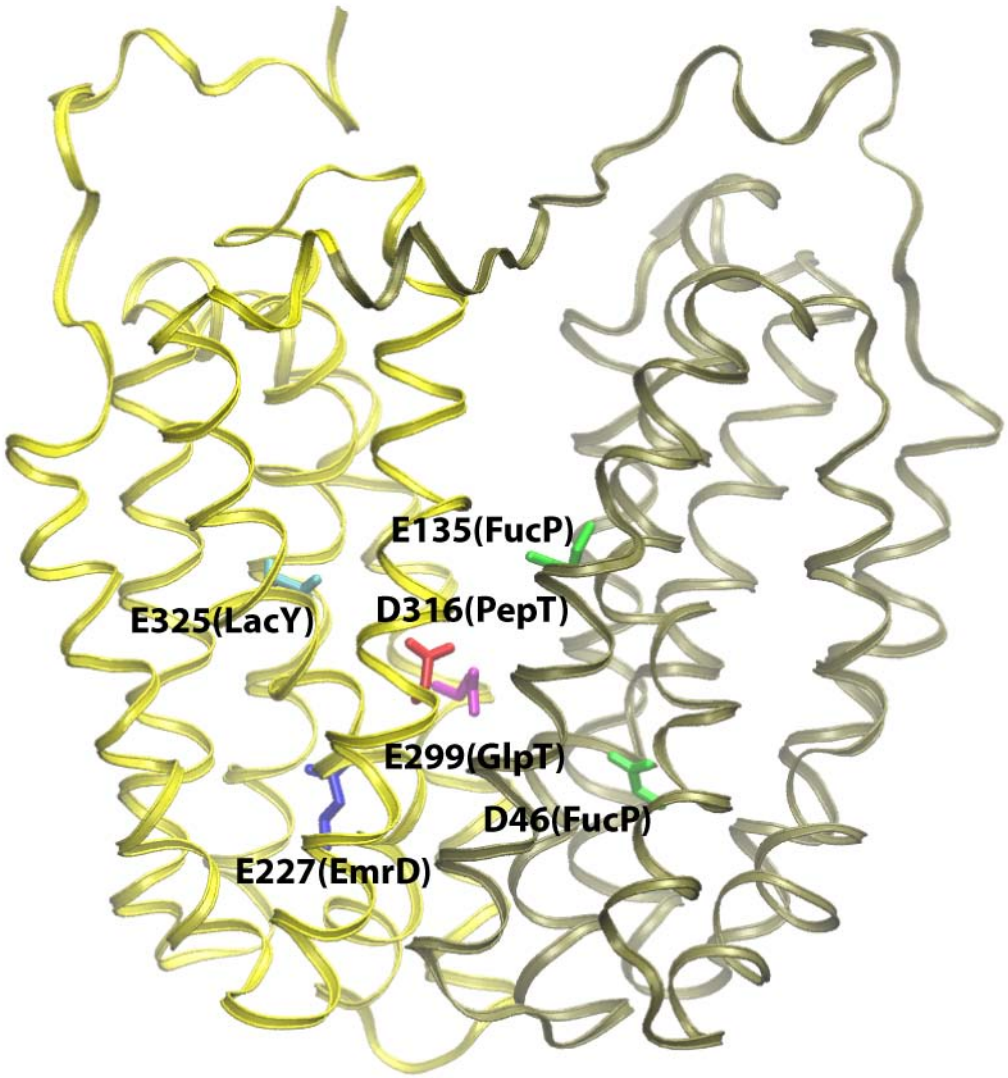

Figure S10, related to Figure 2. The location, relative to Glu325 in LacY (PDB ID 2V8N), of conserved, protonation-sensitive amino acid residues in structurally determined MFS transporters; Asp316 in PepT (PDB ID 2XUT), Glu227 in EmrD (PDB ID 2GFP), Asp46 and Glu135 in FucP (PDB ID 3O7P) and Glu299 in GlpT (PDB ID 1PW4). Multiple sequence alignments were performed using the VMD MultiSeq plugin (Roberts et al., 2006).

References

Olsson, M.H.M., Sondergaard, C.R., Rostkowski, M., and Jensen, J.H. (2011). PROPKA3: Consistent Treatment of Internal and Surface Residues in Empirical pKa Predictions. J. Chem. Theor. Comput. *7*, 525-537.

Roberts, E., Eargle, J., Wright, D., and Luthey-Schulten, Z. (2006). MultiSeq: unifying sequence and structure data for evolutionary analysis. BMC Bioinformatics *7*, 382.

Smart, O.S., Goodfellow, J.M., and Wallace, B.A. (1993). The pore dimensions of gramicidin A. Biophys J *65*, 2455-2460.

Smirnova, I., Kasho, V., Choe, J.-Y., Altenbach, C., Hubbell, W.L., and Kaback, H.R. (2007). Sugar binding induces an outward facing conformation of LacY. Proc. Natl. Acad. Sci. U.S.A. *104*, 16504-16509.

Sorgen, P.L., Hu, Y.L., Guan, L., Kaback, H.R., and Girvin, M.E. (2002). An approach to membrane protein structure without crystals. Proc. Natl. Acad. Sci. U.S.A. *99*, 14037-14040.